Available online at www.sciencedirect.com
SCIENCE DIRECT®
International Journal of Solids and Structures 43 (2006) 3185–3196
INTERNATIONAL JOURNAL OF SOLIDS and STRUCTURES
www.elsevier.com/locate/ijsolstr

Identification of the tensile force in high-tension bars using modal sensitivities

Sooyong Park [a], Sanghyun Choi [b,*], Soon-Taek Oh [c], Norris Stubbs [d], Hwa-Cheol Song [e]

[a] School of Architecture, Youngsan University, Junam-Ri, Ungsang-Up, Yangsan-Si, Kyungnam 626-847, Republic of Korea
[b] Structural Systems and Site Evaluation Department, Korea Institute of Nuclear Safety, Guseong-Dong, Yuseong-Gu, Daejeon 305-600, Republic of Korea
[c] Department of Structural Engineering, Seoul National University of Technology, Gongreung2-dong, Nowon-Gu, Seoul 139-743, Republic of Korea
[d] Department of Civil Engineering, Texas A&M University, College Station, TX 77843, USA
[e] Division of Architecture, Korea Maritime University, Dongsam-Dong, Yeongdo-Ku, Pusan 606-791, Republic of Korea

Received 11 February 2005; received in revised form 28 June 2005
Available online 2 September 2005

Abstract

In certain field applications involving the repair or replacement of structural members, the knowledge of the tensile forces in tension members may be critical in the selection of the retrofit or rehabilitation process. To date, several methods have been presented to estimate in situ tensile forces using static and/or dynamic responses of the tension members. However, each and every one of these methods has its disadvantages as well as advantages in its procedures, level of accuracy, and equipment requirements. This paper presents a practical method to identify the tensile force in a high-tension bar using the changes in the modal sensitivities. The methodology can identify not only the tensile force but also other related parameters such as the magnitude of end constraint. The methodology utilizes the sensitivity relationship between the natural frequencies, the structural parameters, and the tensile force in the member. In this paper, the basic elements of the approach are summarized and the proposed method is validated using both numerical and experimental data. Also, the impact of model uncertainty to the performance of the parameter identification is investigated.

Keywords: Tensile force; High-tension bar; Modal sensitivity; Natural frequency

* Corresponding author. Tel.: +82 42 868 0666; fax: +82 42 868 0523.
E-mail addresses: sypark@ysu.ac.kr (S. Park), schoi@kins.re.kr (S. Choi), alicia@snut.ac.kr (S.-T. Oh), nstubbs@civil.tamu.edu (N. Stubbs), song@mail.hhu.ac.kr (H.-C. Song).

0020-7683/$ - see front matter
doi:10.1016/j.ijsolstr.2005.06.089

1. Introduction

High-tension bars are utilized in the construction of various civil engineering structures including bridges, buildings, and other critical structures. Often for some structures, accurately estimating the tensile force in a member may be extremely important. For example, the restoration, structural strengthening, as well as monitoring of ancient buildings requires the assessment of the forces acting in the tie-bars used to support masonry arches and vaults (Bati and Tonietti, 2001). Therefore, a practical and reliable methodology that can be used to accurately and rapidly assess the tensile forces in such members is of fundamental importance.

To date, several methodologies for determining the tensile force in high-tension members have been proposed in the literature. Shinke et al. (1980) presented a vibration method that measures the tensile force using natural frequencies. While their method is simple and speedy, it has a limitation to the members which is not slender or not sufficiently tensioned. Later Hiroshi et al. (1996) supplemented Shinke et al.'s method with a formula for not slender members. Croci et al. (1988) proposed a static procedure using vertical displacements and the strains. However, the method uses vertical displacements due to progressively increasing loads applied at different points, which are not easily applicable to real structures, of the member. Kyska et al. (1991) proposed a method that utilizes the vibrating chord theory for estimating the tensile force. The method obtains the tensile force from the member's natural frequency, the mass and the real length. In their study, the method has been successfully applied to relatively short cables with simple anchoring devices. However, as the anchorage devices become complicated, determining the member's real vibrating length is difficult. Also, their method has limitation in applying to other tension members with bending stiffness due to the anchoring device and/or the section. Some researchers have proposed combination methods that synthesize other information such as experimental techniques and static measurements with frequency information. Blasi and Sorace (1994) proposed a method that utilizes the vertical displacement and the fundamental frequency. Their method can be applied to a member with unknown boundary conditions by adopting system identification procedures (Sorenson, 1980). Casas (1994) presented a least square minimization approach that combines frequency information with other experimental techniques (strain gauges, pressure in tensioning jacks). Recently, Bati and Tonietti (2001) proposed a static procedure for estimating the tensile force in a metallic tie-rod inserted into a masonry building.

Overall, even with the cumulative efforts presented by many researchers, each and every one of the proposed methods continues to exhibit one or more of the following shortcomings. First, more than one experimental technique is required to yield acceptable estimations of the tensile force (Blasi and Sorace, 1994; Casas, 1994). Second, identification of other parameters, such as the magnitudes of constraints (which is essential for appropriate modeling of some tensile members) are not considered in the formulation of the tensile force determination (Shinke et al., 1980; Croci et al., 1988; Kyska et al., 1991). Third, the practical application of these methods is not computationally straightforward (Croci et al., 1988; Bati and Tonietti, 2001). Finally, in the dynamic-response-based methods, other useful information, such as frequencies of higher modes, is discarded (Blasi and Sorace, 1994).

In this paper, a straightforward and practical methodology for estimating the tensile force in a tension member is presented. The proposed methodology cannot only identify the tensile force but also identify other parameters such as the magnitude of the end constraint. The sensitivity relationship between the parameters, including the axial force and the stiffness parameters, and the natural frequencies is derived from an established sensitivity approach to system identification (Stubbs and Osegueda, 1990; Choi et al., 2004). The proposed sensitivity method is first validated using numerical data from a beam structure. Then, the impact of model uncertainty to the performance of the parameter identification is investigated. Finally, experimental verification is performed using laboratory test data from a bar.

2. Theory

Consider a bar member subjected to an axial load P. Suppose that the member has r elements with q discrete masses. Let λ_i $(i=1,\ldots,n)$ represent the identifiable eigenvalues of a structure; let m_n $(n=1,\ldots,q)$ represent the nth discrete mass of the member; and let k_j $(j=1,\ldots,r)$ represent the stiffness of the jth structural element. If we assume that the mass of bar remains constant, then

$$\lambda_i = \lambda_i(k_1,\ldots,k_r;m_1,\ldots,m_q;P) \tag{1}$$

and

$$\delta\lambda_i = \sum_{j=1}^{r} \frac{\partial\lambda_i}{\partial k_j}\delta k_j + \frac{\partial\lambda_i}{\partial P}\delta P \tag{2}$$

where $\delta\lambda_i$ is the variation in the ith eigenvalue, δk_j is the variation in the stiffness of the jth element, and δP is the variation in the axial load P.

Dividing both sides of Eq. (2) by λ_i and setting $Z_i = \delta\lambda_i/\lambda_i$, then

$$Z_i = \frac{\delta\lambda_i}{\lambda_i} = \sum_{j=1}^{r} \frac{1}{\lambda_i}\frac{\partial\lambda_i}{\partial k_j}\delta k_j + \frac{1}{\lambda_i}\frac{\partial\lambda_i}{\partial P}\delta P = \sum_{j=1}^{r} \frac{k_j}{\lambda_i}\frac{\partial\lambda_i}{\partial k_j}\frac{\delta k_j}{k_j} + \frac{P}{\lambda_i}\frac{\partial\lambda_i}{\partial P}\frac{\delta P}{P} \tag{3}$$

If K_i and M_i are, respectively, the ith modal stiffness and the ith modal mass, substituting $\lambda_i = K_i/M_i$ into Eq. (3) and simplifying yields

$$Z_i = \frac{\delta\lambda_i}{\lambda_i} = \sum_{j=1}^{r} F_{ij}\alpha_j + H_i\psi \tag{4}$$

where $F_{ij} = \frac{k_j}{K_i}\frac{\partial K_i}{\partial k_j}$, $H_i = \frac{P}{K_i}\frac{\partial K_i}{\partial P}$, $\alpha_j = \frac{\delta k_j}{k_j}$, and $\psi = \frac{\delta P}{P}$. If we define

$$Z = \{z_1, z_2, \ldots, z_n\}, \quad \alpha = \{\alpha_1, \alpha_2, \ldots, \alpha_r\}, \quad \psi = \{\psi_1\} \tag{5}$$

and

$$F = \lfloor F_{ij} \rfloor \quad H = \{H_1, H_2, \ldots, H_n\} \tag{6}$$

where F is $n \times r$ matrix and H is $n \times 1$ matrix, Eq. (4) can be written as

$$Z = F\alpha + H\psi \tag{7}$$

Note that Eq. (7) is the basic sensitivity equation.

If the basic equation is rewritten in a partitioned form as

$$Z = F\alpha + H\psi = [F|H]\begin{Bmatrix} \alpha \\ \psi \end{Bmatrix} = A\gamma \tag{8}$$

where F is an $n \times r$ stiffness sensitivity matrix determined from a theoretical model of the bar, H is an $n \times 1$ axial force sensitivity matrix determined from a theoretical model of the bar, Z is an $n \times 1$ matrix containing the fractional changes in eigenvalues between the two systems, α is a $r \times 1$ matrix containing unknown stiffness adjustments, and ψ is a scalar containing unknown axial force adjustments. Then stiffness and axial force adjustments can be determined from the equation

$$\gamma = \begin{Bmatrix} \alpha \\ \psi \end{Bmatrix} = A^{-1}Z \tag{9}$$

where A^{-1} is the generalized inverse.

For steel bars, the geometric parameters can be easily assessed and the material's elastic properties can be evaluated or estimated with less uncertainty. On the other hand, the magnitude of the end constraint, which is essential for appropriate modeling in assessing the member's axial force, is very difficult to identify. However, modeling the constraint as an elastic spring and applying Eq. (9) can give the way to identify the constraint level with only a few numbers of measured frequencies available in field application.

Recall that

$$Z = A\gamma \tag{10}$$

In order to generate the elements of the sensitivity matrix A with the limited number of frequencies, the following procedure is used (Fig. 1):

(1) Assume an initial model of the structure to be identified and compute λ_i $(i = 1,\ldots,n)$ for that structure;
(2) Set a single $\gamma_k = \gamma$ and set all other $\gamma_j = 0$ (i.e., $j \neq k$);
(3) Compute λ_i^* $(i = 1,\ldots,n)$ of the structure to be identified;
(4) Compute eigenvalue sensitivities $Z_i = \delta\lambda_i/\lambda_i$ $(i = 1,\ldots,n)$ where $\delta\lambda_i = \lambda_i^* - \lambda_i$;
(5) Compute the ikth element of the A matrix using the result $A_{ik} = Z_i/\gamma$; and
(6) Repeat for $k = 1,\ldots,r$.

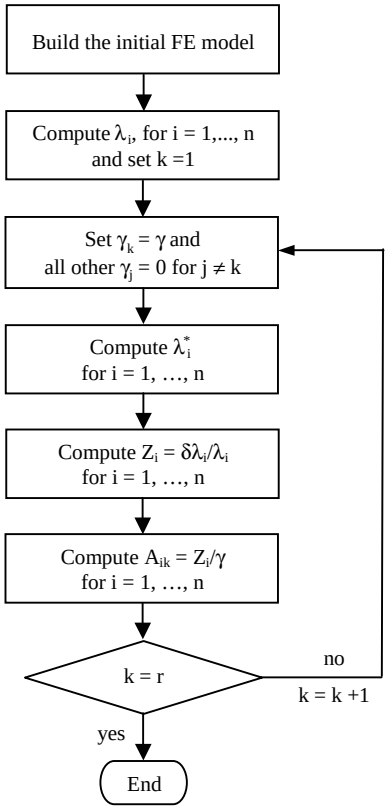

Fig. 1. A procedure for building the sensitivity matrix.

Now having been proposed a method to compute the elements of the sensitivity matrix A, the general identification procedure can be accomplished using the following steps:

(1) Develop an initial FE model for the target member;
(2) Compute the sensitivity matrix A from the FE model;
(3) Compute the fractional changes in eigenvalues, Z, between the FE model and the target member;
(4) Solve Eq. (9) for γ using generalized inverse technique;
(5) Update the spring stiffness and axial force of the FE model using the relationships $k_j^* = k_j(1 + \alpha_j)$ and $P^* = P(1 + \psi)$; and
(6) Repeat Steps (2)–(5) until convergence (i.e., $\alpha_j \approx 0$ and $\psi \approx 0$).

3. Numerical verification

The feasibility of the proposed algorithm is first examined via a numerical example of a bar member subjected to an axial force as shown in Fig. 2. The 2 cm diameter bar is supported by rotational springs at both ends that represent the constraint effect by anchoring devices. The material properties for the target structure are the mass density of 7850 kg/m^3 and the elastic modulus of 1.9×10^4 kN/cm^2. Two-node cubic beam elements are used to model the example structure. The model has 15 elements and 16 nodes. The modal parameters including the natural frequencies and the corresponding mode shapes are obtained via free vibration analysis using SAP2000® (1998).

Table 1 shows the parametric case studies conducted here, which are: slenderness ratio (length/(radius of gyration)) of 200 and 1000 (short and long bars); rotation spring constant of 10 N m and 1000 N m (low and high constraint effects); and tensile force of 10 kN and 100 kN (low and high tensile forces). Using the combinations of the stated parameters, total of 8 target structures are considered. Note that to simplify the problem the spring constants for both ends are assumed to be identical for target structures 1 through 8,

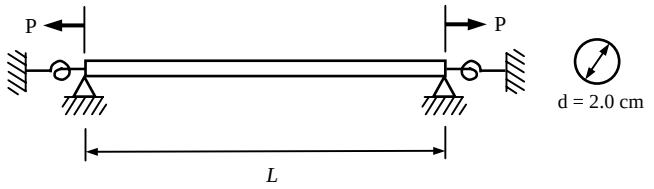

Fig. 2. A beam structure with end rotational springs.

Table 1
Parameters for the target structures

Target structure	Spring constant (N m)	Slenderness ratio (L/r)	Tensile force (kN)
1	10	200	10
2			100
3		1000	10
4			100
5	1000	200	10
6			100
7		1000	10
8			100

which is a reasonable hypothesis for most cases (Blasi and Sorace, 1994). To investigate the robustness of the presented parameter identification technique, the following initial values of the applied tensile force and the rotational spring constant are assumed as a starting point:

(1) *Case A*—the initial assumed values are 10% less than the true values;
(2) *Case B*—the initial assumed values are 50% less than the true values;
(3) *Case C*—the initial assumed values are 300% higher than the true values.

With the obtained natural frequencies, the identification procedure consists of the following three steps: (1) extract natural frequencies from the initial finite element (FE) model, (2) generate stiffness and force sensitivities using the FE model, and (3) update the parameters of the FE model using the procedure outlined in the preceding section. In this example, the parameters to be identified are the tensile force applied to the structure and the spring constants of the end rotational springs. The other sectional and material properties of the initial model are assumed to be identical to the target structure. In the identification, three natural frequencies are utilized and the threshold relative error used is 10^{-4}%. Thus, when the relative error between the frequencies or the identified parameters of the two consecutive steps is less than 10^{-4}%, the iteration is stopped. The convergence of the identification scheme is demonstrated in Tables 2–4 for Cases 1A, 1B, and 1C, respectively. Here, "1A" means that Target structure 1 is identified with 10% less initial values (Case A). In the tables, it can be seen that after just two iterations the differences in the corresponding three frequencies of the identified structure and the target structures are close to 0%.

Table 2
Convergency of the proposed method for Case 1A

Mode	Frequency of initial FE model	Updated frequencies (Hz)		Frequency of target structure	Error (%)	
		Iteration 1	Iteration 2		Initial	Final
1	49.087	50.118	50.117	50.117	2.06	0.00
2	165.752	166.974	166.973	166.973	0.73	0.00
3	358.188	359.457	359.457	359.457	0.35	0.00

Table 3
Convergency of the proposed method for Case 1B

Mode	Frequency of initial FE model	Updated frequencies (Hz)		Frequency of target structure	Error (%)	
		Iteration 1	Iteration 2		Initial	Final
1	44.734	50.132	50.117	50.117	10.7	0.00
2	160.775	166.978	166.973	166.973	3.71	0.00
3	353.070	359.459	359.457	359.457	1.78	0.00

Table 4
Convergency of the proposed method for Case 1C

Mode	Frequency of initial FE model	Updated frequencies (Hz)		Frequency of target structure	Error (%)	
		Iteration 1	Iteration 2		Initial	Final
1	67.585	50.153	50.117	50.117	34.9	0.00
2	189.790	166.984	166.973	166.973	13.7	0.00
3	383.960	359.461	359.456	359.457	6.78	0.00

Table 5
Identified parameters for the beam structure

Case	Number of iterations	Spring constants (N m)			Tensile force (kN)		
		Target	Identified	Error (%)	Target	Identified	Error (%)
1A	2	10	10.03	0.3	10	10.00	0.0
1B	2		9.98	0.2	10	10.00	0.0
1C	2		9.99	0.1	10	10.00	0.0
2A	2		10.00	0.0	100	100.0	0.0
2B	2		10.00	0.0	100	100.0	0.0
2C	2		10.00	0.0	100	100.0	0.0
3A	2		10.00	0.0	10	10.00	0.0
3B	2		10.00	0.0	10	10.00	0.0
3C	2		10.00	0.0	10	10.00	0.0
4A	2		10.00	0.0	100	100.0	0.0
4B	3		10.00	0.0	100	100.0	0.0
4C	2		10.00	0.0	100	100.0	0.0
5A	2	1000	1000.0	0.0	10	10.00	0.0
5B	3		1000.0	0.0	10	10.00	0.0
5C	3		1000.0	0.0	10	10.00	0.0
6A	2		1000.0	0.0	100	100.0	0.0
6B	3		1000.0	0.0	100	100.0	0.0
6C	3		1000.0	0.0	100	100.0	0.0
7A	2		1000.0	0.0	10	10.00	0.0
7B	3		998.0	0.2	10	10.00	0.0
7C	3		999.0	0.1	10	10.00	0.0
8A	2		1000.0	0.0	100	100.0	0.0
8B	3		1000.0	0.0	100	100.0	0.0
8C	3		999.0	0.1	100	100.0	0.0

The results of the parameter identification for eight different target properties are summarized in Table 5. In the table, it is observed that the spring constants and the applied tensile force for all target structures are successfully identified in only a few iterations. Thus, it shows that the proposed identification scheme is independent of the assumed initial properties.

4. Impact of model uncertainty

In field applications, it is expected that there would be some deviations due to uncertainties in measurement data and structural properties (i.e., material and sectional properties). In this section, the impact of the uncertainties to the parameter identification is assessed using the same numerical model utilized in the experimental study, i.e., Section 5. The tension bar is 3.8 m long with 1.8 cm diameter. The applied tensile force and the end-spring constants are arbitrarily chosen as 25 kN and 5 kN m, respectively. Two model-uncertainty types that may exist in the bar model are selected. The first type is the uncertainty associated with the identified natural frequencies. This type of uncertainty may arise when a true natural frequency locates between two frequency responses. The second type selected is the uncertainty in the structural parameters of the bar. This may include (1) errors in the stiffness parameters; (2) errors in the mass parameters; and (3) errors in the damping parameters.

The first uncertainty is simulated by considering the frequency resolution in real applications. In this study, 0.25 Hz, which is the same frequency resolution in the experimental study, is adopted for the Δf. Using the frequency resolution, two different uncertainty cases, Cases U1 and U2, are simulated as follows:

Table 6
Identified parameters for the beam structure with model uncertainty

Case	Simulated deviation (%)		Spring constants (kN m)			Tensile force (kN)		
	Frequency	Stiffness	Target	Identified	Error (%)	Target	Identified	Error (%)
U0	0.0	0.0	5.00	5.00	0.0	25.0	25.0	0.0
U1	0.1			4.99	0.2		25.0	0.0
U2	0.8			5.39	7.8		24.8	0.8
U3		1.0		4.99	0.2		25.0	0.0
U4		10.0		5.39	7.8		24.8	0.8

approximating the target natural frequencies to nearest frequency response values which are multiples of Δf (Case U1); and further adding $+\Delta f$ to the natural frequencies of Case U1 (Case U2).

The uncertainty in the structural parameters is simulated by adding small deviation to the stiffness of the target structure. In this paper, among the stated uncertainties in the structural parameters, only the deviation in the stiffness parameter is considered in the numerical study because: (1) the mass can be evaluated with much less uncertainty; (2) the effect of the mass change to the vibration characteristics can be effectively inferred from the effect of the stiffness change; and (3) the effect of the damping change to the resonant frequencies is negligibly small in general. Two different uncertainty cases, Cases U3 and U4, are simulated as follows: increasing the elastic modulus of the target structure by 1% (Case U3); increasing the elastic modulus of the target structure by 10% (Case U4). Note that the 10% deviation is selected assuming that the coefficient of variation (COV) of the elastic modulus is 0.05 (the maximum COV of the elastic modulus from the literature (Galambos and Ravindra, 1978) is 0.06). Note also that, to simulate the real applications, the frequencies utilized in the parameter identification are approximated to the nearest frequency response values like Cases U1 and U2.

The parameter identifications were performed with 20% lower initial values than the true values, i.e., 20 kN for the tensile force and 4 kN m for the rotational spring constants. The parameter identification results for Cases U0 through U4 are presented in Table 6. Note that Case U0 represents the case without frequency or stiffness deviation. In the table, it can be seen that both the spring stiffness and the tensile force are identified successfully when no deviation presents. With 0.1% deviation in the frequencies, i.e., Case U1, small identification errors can be seen in the identified spring stiffness. In Case U2, the identification error for the spring constant increases to 7.8% while the error for the tensile force stands at 0.8%. The same phenomenon can be observed in Cases U3 and U4. Note that Cases U1 and U3 yield the same identification results due to the frequency approximation process mentioned above. The same results are observed in Cases U2 and U4 due to the same reason. The other notable observation is that 10% stiffness deviation, i.e., Case U4, yields the same error as Case U2 when the deviation in the frequencies is 0.8%. This says that, for tension members, the uncertainty in structural parameters has much smaller impact on the accuracy of the parameter identification than the uncertainty in natural frequencies.

5. Experimental verification

In this section, the feasibility and practicality of the proposed scheme is further demonstrated using the laboratory testing data from a high-tension bar. A laboratory dynamic testing is conducted on a high-tension bar. Fig. 3 shows the high-tension bar utilized in the testing along with the supporting frame structure. The 1.8 cm diameter bar with the length of 3.8 m is pin-connected to the frame and subjected to the tensile forces of 27.3 kN, 32.8 kN, and 41.0 kN designated here as Cases 1, 2, and 3, respectively.

Fixed response measurement testing with roving hammer impacts is performed to collect dynamic response data. One accelerometer is glued to the bar and a total of 7 impact points are marked on the

Fig. 3. A high-tension bar used in the laboratory experiment.

bar to insure the repeatability during the testing. The impact and sensor locations are depicted in Fig. 4. Instrumentation used to conduct the modal test consists of an impact hammer, an ICP accelerometer, an FFT analyzer, and a potable computer. Table 7 tabulates the instrumentation and test settings used for the modal testing. Seven frequency response functions (FRFs) are measured for each case. Five impacts are recorded at each point and an averaged FRF is computed for each impact point. A standard modal analysis (Ewins, 1986) is performed on the collected data set of transfer functions and modal parameters

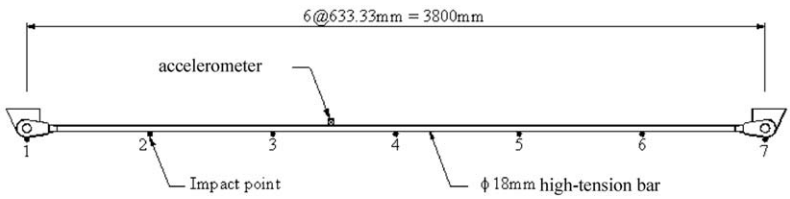

Fig. 4. Locations of the impact points and the accelerometer.

Table 7
Modal test parameters for the test

Parameter	Setting	Notes/Units
Sample frequency	100	Hz
Sample length	400	Samples per channel
Spectral resolution	0.25	Hz
Number of repetitions	5	Linear average
Channel gain	Varied	Set to maximize resolution
Trigger method	+ 18% hammer FS	Pre-trigger save all channels
Accelerometer window	Exponential	99% down at end
Hammer window	Rectangular	7% window width

for the structure are extracted. Table 8 presents the measured natural frequencies for the first three bending modes for Cases 1 through 3, and the corresponding mode shapes are depicted in Fig. 5 for Case 1.

The same identification procedure as stated in the preceding section is used to identify unknown parameters. As a first step, an initial FE model is constructed. The FE model has 16 nodes and 15 cubic beam elements. To investigate the boundary constraint effect as well as the tensile force applied, two identical rotational springs are provided at both ends of the FE model like in Fig. 2. Thus, the parameters to be identified here are the tensile force and the rotational spring constant. In this case, however, since the bar is connected to the frame with pins, it is anticipated that the predicted magnitude of the spring constants should be small numbers. For all three cases, the initial tensile force and the spring constant are assumed to be 30 kN and 10 N m, respectively. A relatively low initial value is selected for the end rotational spring constant, because the bar is pin-connected to the frame as shown in Fig. 3. Other material properties assigned to the initial structure are the mass density (7850 kg/m^3) and the elastic modulus (1.9×10^4 kN/cm^2). The free-vibration analyses are performed using SAP2000® (1998).

Table 8
Natural frequencies of the high-tension bar

	Frequency (Hz)		
	1st mode	2nd mode	3rd mode
Case 1	15.25	30.75	48.50
Case 2	17.00	33.75	53.25
Case 3	19.25	38.00	59.50

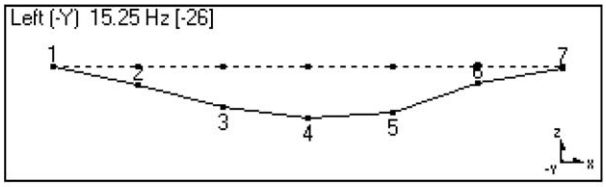

(a) 1st mode

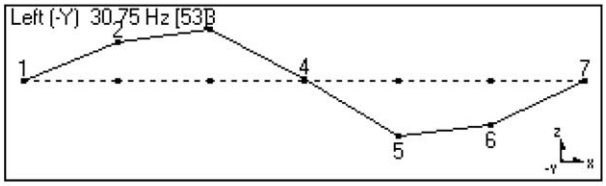

(b) 2nd mode

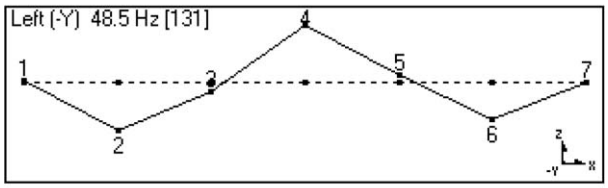

(c) 3rd mode

Fig. 5. Mode shapes of the high-tension bar.

In the parameter identification exercise, three natural frequencies are utilized and the threshold relative error used is selected to be 10^{-2}%. Tables 9–11 show the convergence of the proposed method to the target frequencies. Note that after three iterations the maximum difference between the frequency of the updated FE model and the target structure is 2.08%. The results of the parameter identification for three different target properties, the applied tensile forces, are summarized in Table 12. In the table, it can be seen that as expected the identified spring constants are very small as expected. Although no measured values are provided for the spring constants, the table clearly shows that the identified spring constant increases as the tensile force increases. This trend is reasonable since an increase in tensile force causes an increase in frictional resistance at the pin connections. In the table, it is also observed that the maximum percentage error between the identified and the target forces is 3.66% for Case 1. The difference between the identified and the target values may be attributed to measurement noise, error in modal analysis, and/or other uncertain-

Table 9
Convergency of the proposed method for the high-tension bar (Case 1)

Mode	Frequency of initial FE model	Updated frequencies (Hz)			Frequency of target structure	Error (%)	
		Iteration 1	Iteration 2	Iteration 3		Initial	Final
1	16.09	15.02	14.97	14.98	15.25	5.51	1.77
2	33.00	31.11	31.02	31.02	30.75	7.32	0.88
3	51.88	49.23	49.11	49.11	48.50	6.97	1.26

Table 10
Convergency of the proposed method for the high-tension bar (Case 2)

Mode	Frequency of initial FE model	Updated frequencies (Hz)			Frequency of target structure	Error (%)	
		Iteration 1	Iteration 2	Iteration 3		Initial	Final
1	16.09	16.86	16.71	16.71	17.00	5.35	1.71
2	33.00	34.68	34.40	34.40	33.75	2.22	1.93
3	51.88	54.39	53.99	53.99	53.25	2.57	1.39

Table 11
Convergency of the proposed method for the high-tension bar (Case 3)

Mode	Frequency of initial FE model	Updated frequencies (Hz)			Frequency of target structure	Error (%)	
		Iteration 1	Iteration 2	Iteration 3		Initial	Final
1	16.09	19.09	18.85	18.85	19.25	16.42	2.08
2	33.00	39.03	38.57	38.57	38.00	13.16	1.50
3	51.88	60.65	59.99	59.99	59.50	12.81	0.82

Table 12
Identified parameters for the high-tension bar

Case	Number of iterations	Spring constants (N m)	Tensile force (kN)		
		Identified	Target	Identified	Error (%)
1	3	0.20	27.3	26.3	3.66
2	3	0.28	32.8	31.9	2.74
3	3	0.93	41.0	41.2	0.49

ties. One notable observation from the result is that as the magnitude of the applied force increases, the relative error decreases.

6. Conclusions

In this paper, a sensitivity-based methodology for identifying the tensile force in structural members such as high-tension bars was presented. The methodology utilized the dynamic sensitivity relationship between the natural frequencies, the applied tensile force, and the stiffness properties of the member. The feasibility of the methodology was demonstrated using simulated data from a pin-pined beam with rotational springs. The practicality of the method was demonstrated with experimental data obtained from a high-tension bar.

From the numerical and experimental studies, the following conclusions are drawn:

1. The numerical simulation of a bar reveals that the proposed methodology can identify applied tensile forces and constraint parameters with negligible errors;
2. The model uncertainty study shows that the identified tensile force is less vulnerable than the identified end constraint effects to the uncertainty associated with natural frequency and structural parameters;
3. The model uncertainty study reveals that, for tension members, the uncertainty in structural parameters has less impact on the accuracy of the parameter identification than the uncertainty in natural frequencies;
4. The experimental study shows that the proposed methodology can identify applied tensile forces with very small errors; and
5. From the numerical and the experimental studies, the proposed sensitivity-based method is a feasible approach to identify the resulting tensile force and the end constraint effects in tensionally loaded members.

References

Bati, S.B., Tonietti, U., 2001. Experimental methods for estimating in situ tensile force in tie-rods. Journal of Engineering Mechanics 127 (12), 1275–1283.

Blasi, C., Sorace, S., 1994. Determining the axial force in metallic rods. Structural Engineering International 4 (4), 241–246.

Casas, J.R., 1994. A combined method for measuring cable forces: the cable-stayed Alamillo Bridge, Spain. Structural Engineering International 4 (4), 235–240.

Choi, S., Park, S., Bolton, R., Stubbs, N., Sikorsky, C., 2004. Periodic monitoring of physical property changes in a concrete boc-girder bridge. Journal of Sound and Vibration 278 (1–2), 365–381.

Croci, G., Buliani, G., Ascensig, G., 1988. Studies and experimentation on the Ludovisi Cloister in Rome. In: Third Congress of the Italian Association for Restoration and Strengthening of Constructions, Cataia, Italy. pp. 305–315.

Ewins, D.J., 1986. Modal Testing: Theory and Practice. Research Studies Press, Hertfordshire, England.

Galambos, T.V., Ravindra, M.K., 1978. Properties of steel for use in LRFD. Journal of the Structural Division 104 (ST9), 1459–1468.

Hiroshi, Z., Shinke, T., Namita, Y., 1996. Practical formulas for estimation of cable tension by vibration methods. Journal of Structural Engineering 122 (6), 651–656.

Kyska, R., Koutny, V., Rosko, P., 1991. Tension measurement in cable of cable-stayed bridges and in free cables. In: Proceedings of the Second Conference on Traffic Effects on Structures and Environment, Zilina, Slovakia. pp. 190–194.

SAP2000, 1998. User's Manual. Computers and Structures, USA.

Shinke, T., Hironaka, K., Zui, H., Nishimura, H., 1980. Practical formulas for estimation of cable tension by vibration methods. Proceedings of JSCE 294, 25–34.

Sorenson, H.W., 1980. Parameter Estimation. Marcel Dekker Ed., New York.

Stubbs, N., Osegueda, R., 1990. Global non-destructive damage evaluation in solids. The International Journal of Analytical and Experimental Modal Analysis 5 (2), 67–79.